Quantized ionic conductance in nanopores

Michael Zwolak[1], **Johan Lagerqvist**[2], and **Massimiliano Di Ventra**[2]

[1]Theoretical Division, MS-B213, Los Alamos National Laboratory, Los Alamos, NM 87545

[2]Department of Physics, University of California, San Diego, La Jolla, CA 92093

Abstract

Ionic transport in nanopores is a fundamentally and technologically important problem in view of its occurrence in biological processes and its impact on novel DNA sequencing applications. Using microscopic calculations, here we show that ion transport may exhibit strong nonlinearities as a function of the pore radius reminiscent of the conductance quantization steps as a function of the transverse cross section of quantum point contacts. In the present case, however, conductance steps originate from the break up of the hydration layers that form around ions in aqueous solution. Once in the pore, the water molecules form wavelike structures due to multiple scattering at the surface of the pore walls and interference with the radial waves around the ion. We discuss these effects as well as the conditions under which the step-like features in the ionic conductance should be experimentally observable.

Over the last decade there have been tremendous advances in both the fabrication of nanopores and their use for molecular recognition and nucleic acid analysis [1]. Experimental characterization of molecules has mostly relied on measuring changes in the ionic current through the pore [2–5], but other ways to probe single molecules in nanopores may come from embedding nanoscale sensors within the pore or nanochannels [6–13]. However, electronic fluctuations due to the dynamical ionic and aqueous environment will affect the type of signals and noise these sensors detect. Therefore, understanding the electrostatics of ions in water at atomic length scales is crucial in our ability to design functional single-molecule sensors and to interpret their output, and will also provide new insight into the operation of the ubiquitous biological ion channels.

Several studies have examined the electrostatics of ions in nanopores using continuum models for the dielectric properties of water [14–17]. Within a continuum model, the nanopore electrostatic environment is essentially one-dimensional due to the large difference of dielectric constants between water and the surrounding pore material [16]. Thus, according to these models, there is a large electrostatic energy penalty to move an ion from the exterior of the pore to its interior [14,16], with small amounts of surface charge able to drastically reduce this energy penalty [14]. Although continuum models can highlight some generic features of ionic currents and blockades, such as the effect of surface charges, they miss important effects related to the microscopic physical structure of water molecules around ions.

Here, we examine ionic transport from the point of view of these nanoscale features (see schematic in Fig. (1)). Using all-atom molecular dynamics simulations, we calculate the structural and electrostatic details of a single ion in an aqueous environment both in and out of a cylindrical nanopore (see Methods for details). Ions in solution create local structures in the surrounding water, known as *hydration layers* [18], and characterized by oscillations in the water density. The length scales associated with these oscillations and their decay are in the range 2–10 Å, i.e., comparable to the radial dimensions of some nanopores. In addition, we show that when the ion is inside the pore, water molecules form wavelike features due to both the interaction with the walls and the water molecules in the partially broken hydration layers.

Starting with these microscopic considerations, we propose a model system based on the concept of *energy shells*, which incorporates the hydration layer structure into the energetic barrier created by the pore. We predict that the ionic conductance of a nanopore manifests step-like features as a function of the pore radius similar to the quantized conductance of quantum point contacts as a function of their effective cross section (see, e.g., [19]). Finally, we examine the influence of noise on ionic transport and discuss the experimental conditions under which the above step-like features are most likely to be observed.

To be specific, we focus our attention on an isolated chlorine ion but similar considerations will apply to other types of ions and situations. Immediately around the Cl anion, the water molecules orient themselves so that a single hydrogen from each molecule points inward toward the ion (see Fig. (1)). The distribution of water molecules forms into layers as shown in Fig. (2). The inner most layer is very tightly bound, and subsequent layers are spaced at 2.0 – 2.3 Å. These findings are in good agreement with neutron diffraction and X-ray absorption experiments that measure the radial distribution of water [20], which give a Cl-O peak at ~ 3.1 Å, as well as molecular dynamics simulations performed with different force field parameters [21]. In addition, we can acquire further information not directly accessible from experiments, such as the microscopic electric field due to the ions and water (shown in the inset of Fig. (2) (b)). This field shows oscillations corresponding to the hydration layers and is similar to a series of alternating charged surfaces. A continuum picture, however, would not capture these microscopic details that are responsible for the conductance steps we predict.

If the anion is now placed in the nanopore, the hydration layers are affected. For large pores, the hydration layer structure is identical to that in bulk water. However, as the pore is taken to nanoscale dimensions, eventually the pore walls (or effective pore wall, which may be, e.g., a layer of tightly bound water molecules) will force the hydration layer to be partially broken because it can not fit within the pore. Figures 2(c, d) show this effect. Within a 15°A radius pore, the first and second hydration layers are still present. On the other hand, for a 12 Å pore radius, the first layer is still intact, but the second layer is partially broken. Indeed, it is almost a spherical shell cutoff by the effective pore wall which comes at about 5 Å from the axis of the pore. In order to gain physical insight, we propose the following model system that captures this essential aspect of the presence of hydration layers around the ion.

Model System

The hydration layers stay partially intact except for the portion of the hydration surface cut off by the pore walls, i.e., for layers with radii greater than the effective pore radius. In other words, only the portion of the layer along the axis of the pore remains intact. We consider then a set of surfaces placed at each hydration layer, i, at radius R_i. Each surface represents the area where the water dipoles fluctuate, giving the time-averaged dipole layers. Ignaczak et al. [22] have found that for small water clusters around a Cl anion, the internal energy of each water is approximately linear in the number of water molecules in the cluster. Since interactions (van der Waals and electrostatic) with a low dielectric pore are small compared to water-ion and water-water interactions [23], this suggests writing the internal energy contained in a partially intact hydration layer as

$$U_i = f_i U_i^o \tag{1}$$

where f_i is the fraction of the layer present in the pore and U_i^o is the energy difference of that stored in the intact water layer and the water in bulk.

In our model, the energy barrier is due to the stripping off of a fraction of the layer, f_i, i.e., the fraction of a spherical surface at R_i that remains within the pore of effective radius R_p. When the ion translocates along the pore axis, the surface area that remains in layer i is given by

$$S_i = 2\Theta (R_i - R_P) \int_0^{2\pi} d\phi \int_0^{\theta_c} d\theta R_i^2 \sin\theta \tag{2}$$

where $\Theta(x)$ is the step function and $\theta_c = \sin^{-1} R_p/R_i$. When $R_p < R_i$, the fraction of the surface left is

$$f_i(R_P) = 1 - \sqrt{1 - \left(\frac{R_P}{R_i}\right)^2}. \tag{3}$$

The internal energy barrier as function of pore radius is then given by

$$\Delta U(R_p) = \sum_i (f_i(R_p) - 1)U_i^o, \tag{4}$$

where the summation is over the layers. The free energy change of hydration is dominated by the contribution from the total internal energy contained within the hydration layers, $\sum_i U_i^o$, plus a bulk dielectric contribution from water outside the layers. Previous calculations give the total internal energy change in the range −3.5 to −3.7 eV [22,24,25]. The form of the electric field shown in Fig. 2(b) suggests that the time-averaged microscopic distribution of waters can be viewed as a set of spherical layers of alternating charge. Thus, the energy stored within each layer should be well estimated by using a Born solvation calculation, which, by construction, will sum to the total internal energy contribution. The physical content of this calculation is that of the solvation of embedded "quasiparticles": the total solvation energy is given by solvating the ion; the energy of the first layer is the difference of solvating the ion and solvating the ion plus the first layer, i.e., solvating a "quasiparticle" consisting of the ion and a cluster of waters. With this picture in mind, the energy within each layer is given by

$$U_i^o = \frac{e^2}{8\pi\varepsilon_0}\left(1 - \frac{1}{\kappa}\right)\left(\frac{1}{R_i^O} - \frac{1}{R_i^I}\right) \tag{5}$$

where κ is the dielectric constant of water and $R_i^{I(O)}$ are the inner (outer) radii demarcating the hydration layer, and we have used the effective ion charge of $1e$, which is consistent with the field recovering its bare ion value after each hydration layer (see inset of Fig. 2(b)). From the water density oscillations shown in Fig. 2, these radii are 2.0 and 3.9 for the first layer; 3.9 and 6.2 for the second; 6.2 and 8.5 for the third. The total solvation energy is then −3.6 eV and the layer energies are −1.7, −0.7, and −0.3 eV for the first, second, and third layers, respectively. Immediately, we can understand why the third layer is absent within the pore: van der Waals interactions [23] and entropic contributions from the water structure [26] are of the same magnitude.

In addition to the internal energy change, there is also an entropic contribution to the free energy change that comes from removing a single ion from solution and localizing it in the pore. Assuming an ideal ionic solution, this entropic contribution is $\Delta S = k_B \ln (V_p n)$, where V_p is the volume of the pore, n is the bulk ionic concentration, and k_B is the Boltzmann constant.

The final free energy difference, $\Delta F = \Delta U - T\Delta S$, is plotted in Fig. (3). This is the main result of this work: hydration layers hold energy in a shell-like structure that causes step-like features in the energy barrier to ionic transport. These step-like features generate corresponding features in the ionic current shown in Fig. (3).

For the remaining portion of this paper, we discuss the conditions under which these features can be observed experimentally and address how the assumptions we have made affect our conclusions. First, we have assumed that only the single ion barrier is important, i.e., that there are no correlated transport processes. We can obtain an indication of whether experiments are consistent with this assumption by considering the ionic concentration. If the bulk salt concentration is 1 M, a typical ion (counting both anions and cations) will be contained in a volume with linear dimension 9.4 Å. This is large enough to almost house both the first and second hydration layers. Since in the absence of significant surface charge on the pore walls, one expects the ionic concentration within the pore to be lower, a bulk concentration of 1 M is consistent with having ions translocate through the pore independently. A 1 M concentration is likely to be small enough to allow at least the effects of the first ionic layer to be observed, i.e., a sudden drop in the current when the pore radius is comparable to the first hydration layer.

For arbitrary concentrations, the ion-ion distance goes as $\sim 9.4/n_0^{1/3}$ Å. If the ion is to be contained in a linear dimension of 20 Å to allow all hydration layers to be present, then one would want a concentration of about 0.1 M. Low concentrations are therefore key to observe the outermost hydration layers. Furthermore, the ionic concentration itself may be used to observe the step-like features. Namely, at certain concentrations the anion-anion (cation-cation) distance would be small enough so that the hydration layers should break with increasing concentration, and a corresponding nonlinearity would be observed.

Second, we have neglected energetic fluctuations due to other effects present, such as thermal noise, ion-ion inter-action, rough pore surfaces, a distribution of ion paths through the pore, and the fact that hydration layers are not exactly represented by their time-averaged oscillations (therefore, some ions with intact hydration layers could go into pores smaller than the radius R_i would predict). In order to determine how robust the step-like features are to these noise sources, we add in our calculations Gaussian noise in the pore radius. In particular, we define a noise strength parameter ξ (i.e., the standard deviation of the Gaussian noise) to describe both energetic and path fluctuations. In Fig. (3), we plot dI/dR_p as a function of R_p and ξ. For no noise, $\xi = 0$ Å, there are well defined peaks in dI/dR_p. However, at a noise strength of $\xi = 0.2$–0.3 Å, the peaks from the second and third layers are smoothed out. Given the width of the hydration layers as seen in Fig. (2), the effects from the second and third layers may not be observable when transport is due to ions like Cl^-, or K^+. However, other ions, such as the divalent Mg or trivalent Al ions [29,30], as well as some monovalent ions [23], have more strongly bound second and third layers. Together with using tunable properties, such as temperature [25,30], this may allow observing the step-like features in the current. In addition, the noise gives an alternative way to observe the effect of the hydration layers. As shown in Fig. (3)(c), the relative noise peaks when the pore radius is near that of a hydration layer. This effect can be understood in terms of a two-state picture: fluctuations that decrease the pore radius energetically "close" the pore, whereas fluctuations that increase the pore radius "open" the pore, essentially creating an instability in the current. Such an effect could also be induced artificially by sampling over a distribution of pore radii centered around a layer radius. The other features of the relative noise can also be understood within this picture.

Third, we have assumed ion translocation is along the axis of the pore. In reality, the ions can move off center. There are different factors which cause this. First, the hydration layers at any given instant are not spherically symmetric. In fact, some ions have asymmetric hydration layers where at a given time, for instance, the first layer is offset to one side of the ion [22]. However, this fact cannot destroy the effect we predict: in these cases, the hydration layer may

be able to "squeeze" into a smaller radius pore by moving off center, but eventually it has to break in a highly nonlinear way. Another cause, however, is something that our model predicts: if the energy is contained in a spherical layer, then the ion actually tends to move off center. This is a consequence of geometry: more of the spherical surface can fit into the pore if the ion moves toward the pore wall. However, the ion cannot move too far from the center, otherwise some of the inner layers would have to be partly destroyed with consequent energy penalty. Neither of these two causes would change our predictions, although they may change some details, such as at what pore radius the conductance jumps occur. Finally, a strong affinity of the ion for the pore wall may occur, for instance, if the pore were significantly charged. This effect may indeed reduce the energy barrier for ionic transport considerably, making all but the first hydration layer breakup undetectable in the ionic current. The charging of the pore walls, which depends heavily on pore material and treatment [31], as well as other factors, can again be somewhat resolved by observing transport with different ion and pore types.

Before we conclude, we briefly mention the other water patterns within the pore. These patterns depend on pore size - different size pores can give maxima and minima in the water density along the pore axis [32]. Further, we find that when the pore radius is 10 Å (effective radius ~ 3 Å) there is a transition in the water structure of the pore [33–35]. Carefully controlled ionic transport measurements may also be able to detect these changes in addition to the nonlinear features due to the hydration layers.

Conclusions

We have examined ionic transport through nanopores using both molecular dynamics and electrostatic calculations. A simple form of the free energy barrier can capture an important effect of hydration layers - namely that the layers produce step-like features in the energy barrier for ions to enter a nanopore, and thus also the ionic conductance, as a function of pore radius. This effect is the classical counterpart of the electronic quantized conductance one observes in quantum point contacts as a function of their cross section. Like the quantum case, one needs sufficient experimental control of the nanopore characteristics in order to observe this effect. Irrespective, a drop in the current should be observable when the first hydration layer is hit, similar to what is thought to occur in the open and closed states of some biological pores [36–38]. However, under the right conditions, multiple current drops should be observed. Further, the relative noise has a characteristic peak when the pore radius is near a hydration layer radius, and this gives an alternative way to observe the effect of hydration. Due to the growing importance of ionic transport in DNA sequencing, this effect may have consequences for future technologies. In addition, the operation of biological ion channels has many factors associated with it, such as favorable internal sites [39] that compensate for the loss of hydration (favorable interactions can also exist in artificial pores [40,41]) or correlated ionic processes [42]. Thus, investigations with more well-controlled synthetic pores can help shed light on the different factors at play and we hope our work will motivate experiments to specifically examine the role of dehydration.

Methods

The molecular dynamics simulations are performed with the NAMD2 package [43] and the simulation details are as in Refs. [7–9]. The TIP3 [44] model is used for the description of water, which is known to reproduce the dielectric properties of bulk water [45]. For all simulations, a single chlorine anion is taken as fixed since its thermal wavelength at room temperature is ~ 0.2 Å. The cylindrical, Si_3N_4 nanopore surfaces carry a charge of $6 - 8 \times 10^{-4}$ e/atom for the 15 Å and 12 Å radius pores. The density plots for an ion in a spherical droplet of water are calculated by averaging the last 900 out of a 1,000 snapshots (taken at 1 ps intervals) within spherical shells of thickness 1 Å. For an ion inside a pore, the last 4000

out of 5000 snapshots (taken at 0.1 ps intervals) are averaged within cylindrical shells of thickness 1 Å in both the radial and vertical directions. The electric field is calculated by averaging the ion and dipole moment contributions over the snapshots.

Acknowledgments

References

1. Zwolak M, Di Ventra M. Rev. Mod. Phys 2008;80:141.
2. Kasianowicz JJ, Brandin E, Branton D, Deamer DW. Proc. Natl. Acad. Sci. U. S. A 1996;93:13770. [PubMed: 8943010]
3. Akeson M, Branton D, Kasianowicz JJ, Brandin E, Deamer DW. Biophys. J 1999;77:3227. [PubMed: 10585944]
4. Meller A, Nivon L, Brandin E, Golovchenko J, Branton D. Proc. Natl. Acad. Sci. U. S. A 2000;97:1079. [PubMed: 10655487]
5. Vercoutere W, Winters-Hilt S, Olsen H, Deamer D, Haussler D, Akeson M. Nat. Biotechnol 2001;19:248. [PubMed: 11231558]
6. Zwolak M, Di Ventra M. Nano Lett 2005;5:421. [PubMed: 15755087]
7. Lagerqvist J, Zwolak M, DiVentra M. Nano Lett 2006;6:779. [PubMed: 16608283]
8. Lagerqvist J, Zwolak M, Di Ventra M. Biophys. J 2007;93:2384. [PubMed: 17526560]
9. Lagerqvist J, Zwolak M, Di Ventra M. Phys. Rev. E 2007;76:013901.
10. Heng JB, Aksimentiev A, Ho C, Dimitrov V, Sorsch TW, Miner JF, Mansfield WM, Schulten K, Timp G. Bell Labs Technical Journal 2005;10:5. [PubMed: 18815623]
11. Gracheva ME, Xiong A, Aksimentiev A, Schulten K, Timp G, Leburton J-P. Nanotechnology 2006;17:622.
12. Gracheva ME, Aksimentiev A, Leburton J-P. Nanotechnology 2006;17:3160.
13. Liang X, Chou SY. Nano Lett 2008;8:1472. [PubMed: 18416580]
14. Zhang J, Kamenev A, Shklovskii BI. Phys. Rev. Lett 2005;95:148101. [PubMed: 16241693]
15. Kamenev A, Zhang J, Larkin A, Shklovskii B. Physica A 2006;359:129.
16. Teber S. J. Stat. Mech 2005:P07001.
17. Bonthuis DJ, Zhang J, Hornblower B, Mathe J, Shklovskii BI, Meller A. Phys. Rev. Lett 2006;97:128104. [PubMed: 17026003]
18. Hille, B. Ion Channels of Excitable Membranes. Sinauer Associates; 2001.
19. Di Ventra, M. Electrical Transport in Nanoscale Systems. Cambridge: Cambridge University Press; 2008.
20. Ohtaki H, Radnai T. Chem. Rev 1993;93:1157.
21. Yang ZZ, Li X. J. Phys. Chem. A 2005;109:3517. [PubMed: 16839014]
22. Ignaczak A, Gomes JANF, Cordeiro MNDS. Electrochim. Acta 1999;45:659.
23. Yang L, Garde S. J. Chem. Phys 2007;126:084706. [PubMed: 17343468]
24. Chandrasekhar J, Spellmeyer DC, Jorgensen WL. J. Am. Chem. Soc 1984;106:903.
25. Duan Z, Zhang Z. Mol. Phys 2003;101:1501.
26. Robinson, RA.; Stokes, RH. Electrolyte Solutions. Mineola, NY: Dover Publications, Inc.; 1959.
27. Deamer DW, Branton D. Acc. Chem. Res 2002;35:817. [PubMed: 12379134]
28. Ho C, Qiao R, Heng JB, Chatterjee A, Timp RJ, Aluru NR. Proc. Natl. Acad. Sci. U. S. A 2005;102:10445. [PubMed: 16020525]
29. Ikeda T, Boero M, Terakura K. J. Chem. Phys 2007;127:074503. [PubMed: 17718616]
30. Bylaska EJ, Valiev M, Rustad JR, Weare JH. J. Chem. Phys 2007;126:104505. [PubMed: 17362073]
31. Chen P, Mitsui T, Farmer DB, Golovchenko J, Gordon RG, Branton D. Nano Lett 2004;4:1333.

32. Lynden-Bell RM, Rasaiah JC. J. Chem. Phys 1996;105:9266.

33. Hummer G, Rasaiah JC, Noworyta JP. Nature 2001;414:188. [PubMed: 11700553]

34. Zangi R, Mark AE. J. Chem. Phys 2003;119:1694.

35. Carrillo-Tripp M, San-Román ML, Hernández-Cobos J, Saint-Martin H, Ortega-Blake I. Biophys. Chem 2006;124:243. [PubMed: 16765508]

36. Peter C, Hummer G. Biophys. J 2005;89:2222. [PubMed: 16006629]

37. Miyazawa A, Fujiyoshi Y, Unwin N. Nature 2003;423:949. [PubMed: 12827192]

38. Beckstein O, Sansom MSP. Phys. Biol 2004;1:42. [PubMed: 16204821]

39. Gouaux E, MacKinnon R. Science 2005;310:1461. [PubMed: 16322449]

40. Fornasiero F, Park HG, Holt JK, Stadermann M, Grigoropoulos CP, Noy A, Bakajin O. Proc. Natl. Acad. Sci. U. S. A 2008;105:17250. [PubMed: 18539773]

41. Nishizawa M, Menon VP, Martin CR. Science 1995;268:700. [PubMed: 17832383]

42. Bernéche S, Roux B. Nature 2001;414:73. [PubMed: 11689945]

43. Kale L, Skeel R, Bhandarkar M, Brunner R, Gursoy A, Krawetz N, Phillips J, Shinozaki A, Varadarajan K, Schulten K. J. Comput. Phys 1999;151:283.

44. Jorgensen WL. J. Am. Chem. Soc 1981;103:4721.

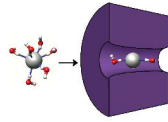45. Simonson T. Chem. Phys. Lett 1996;250:450.

Figure 1.
Schematic of a single anion with its first hydration layer that moves into a nanopore. Due to spatial constraints many water molecules need to be stripped off for the ion to enter the pore, creating nonlinearities in ionic conductance.
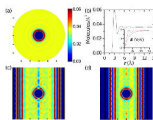
Figure 2.
Water density around a Cl anion both in bulk and inside cylindrical nanopores of different radii. (a) Water density (using the oxygen as the location of the water molecule) around a Cl anion in bulk water. (b) Water density versus radial distance from a Cl anion. At distances greater than 10 Å the water density is approximately 0.036 molecules/$\mathring{A}^3$, which is slightly more than bulk water density of 0.033 molecules/$\mathring{A}^3$ at room temperature. Some edge effects are present around 15 Å. The distribution of water molecules shows oscillations corresponding to the formation of hydration layers, which is also reflected in the electric field. The inset shows the time averaged radial electric field (versus the radial distance) from both the ion and water dipoles (red line) and from just the ion (black dashed line). (c) Water density around a Cl anion inside a 15 Å radius pore (the pore walls are at the edge of the figure). There are wavelike features that are due to interference patterns between oscillations reflecting off the walls of the pore (that set an effective pore radius) and those around the ion. However, the first two layers around the anion are still present. (d) Water density around a Cl anion inside a 12 Å radius pore (the pore walls are indicated by vertical, thick black lines). Here the effective radius is approximately 5 Å, thus the second hydration layer interacts with the effective pore wall and it is partly broken.
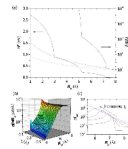
Figure 3.
(a) Free energy barrier to bring an ion into a nanopore and the ionic current at room temperature as a function of the effective pore radius. The dotted red line indicates the ionic current without a free energy barrier and the dashed blue line is the current with just the entropic barrier. The current is calculated at 120 mV and 1 M bulk salt concentration assuming the ionic current is

given by $I = 2\pi R_p^2 e\mu nE$, where the density n is proportional to a Boltzmann factor containing the energy barrier, namely $n = n_0 \exp(-\Delta F/kT)$, with n_0 the bulk salt concentration, μ the ion mobility, and E the strength of the electric field. A typical ion mobility is $\mu = 2.28 \times 10^{-8} m^2/Vs$ (see, e.g., Refs. [27] and [28]). (b) dI/dR_p as a function of pore radius and noise strength. For zero noise, the step-like features in the ionic current give rise to well defined peaks in the derivative of the current. However, as the noise is increased, the peaks smooth out. This occurs beyond a noise strength of $\xi = 0.2 - 0.3$ Å for the second and third layers (see text for details). (c) Relative noise, $\Delta I_{rel} = (\langle I^2\rangle - \langle I\rangle^2)^{1/2}/\langle I\rangle$, versus pore radius for the outermost hydration layer and for $\xi = 0.05, 0.15, 0.25, 0.35, 0.45$. If the pore radius is tuned to the radius of a hydration layer, fluctuations give rise to a peak in the relative noise, which gives an alternative method to observe the effect of the hydration layer.